



Foraging on the potential energy surface: A swarm intelligence-based optimizer for molecular geometry

Christoph Wehmeyer, Guido Falk von Rudorff, Sebastian Wolf, Gabriel Kabbe, Daniel Schärf, Thomas D. Kühne, and Daniel Sebastiani

Citation: *The Journal of Chemical Physics* **137**, 194110 (2012); doi: 10.1063/1.4766821

View online: <http://dx.doi.org/10.1063/1.4766821>

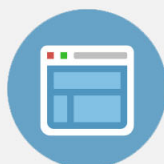
View Table of Contents: <http://scitation.aip.org/content/aip/journal/jcp/137/19?ver=pdfcov>

Published by the [AIP Publishing](http://www.aip.org)



Re-register for Table of Content Alerts

Create a profile.



Sign up today!



Foraging on the potential energy surface: A swarm intelligence-based optimizer for molecular geometry

Christoph Wehmeyer,¹ Guido Falk von Rudorff,¹ Sebastian Wolf,¹ Gabriel Kabbe,¹ Daniel Schärff,² Thomas D. Kühne,² and Daniel Sebastiani^{1,3,a)}

¹*Dahlem Center for Complex Quantum Systems, Freie Universität Berlin, Arnimallee 14, 14195 Berlin, Germany*

²*Institute of Physical Chemistry and Center of Computational Sciences, Johannes Gutenberg University Mainz, Staudinger Weg 9, 55128 Mainz, Germany*

³*Institute of Chemistry, Martin-Luther-University Halle-Wittenberg, von-Danckelmann-Platz 4, 06120 Halle, Germany*

(Received 12 September 2012; accepted 25 October 2012; published online 21 November 2012)

We present a stochastic, swarm intelligence-based optimization algorithm for the prediction of global minima on potential energy surfaces of molecular cluster structures. Our optimization approach is a modification of the artificial bee colony (ABC) algorithm which is inspired by the foraging behavior of honey bees. We apply our modified ABC algorithm to the problem of global geometry optimization of molecular cluster structures and show its performance for clusters with 2–57 particles and different interatomic interaction potentials. © 2012 American Institute of Physics. [<http://dx.doi.org/10.1063/1.4766821>]

I. INTRODUCTION

The prediction of molecular structure by means of numerical calculations represents one of the major fundamental challenges in computational chemistry and physics. The formidable problem of locating the global minimum of the potential energy surface (PES) is a field of intense research, despite the apparent simplicity of the question. Especially the accurate determination of the global minimum structure of complex (bio)molecular systems is known as an extremely difficult task.^{1–5} The multimodal character of the potential energy surface prevents straight minimization pathways; hence, commonly used geometry optimization techniques will converge to the next local minimum structure.

There are several well established approaches to avoid the pitfall of local minima trapping during molecular dynamics simulations, e.g., parallel tempering,⁶ simulated annealing,^{7–9} and metadynamics.^{10–12} For global geometry optimization, a variety of combined minimization and escaping strategies have been proposed, in particular minima hopping,^{13,14} basin hopping,^{15–17} and gradient tabu search,^{18–21} and in recent years, genetic and evolutionary algorithms^{22,23} have been applied to this problem with great success.^{24–33} However, despite the range of methodical approaches, the accurate and feasible prediction of global minima structures is still far from being a routine problem.

In this study, we propose an alternative global optimization approach from the field of swarm intelligence; a field that is yet not widely used in physics and chemistry. The algorithm that we introduce is based on the artificial bee colony (ABC) algorithm,^{34–36} a stochastic approach for global optimization of numerical functions. The basic idea relies on the simultaneous evaluation of a function at different positions by multiple random walkers and an intelligent communication scheme

between the latter to search the function's hypersurface for extrema in a very efficient way—inspired by the foraging behavior of honey bees.

The original artificial bee colony algorithm³⁴ introduces three different types of random walkers: **Scouts** move over the hypersurface in a random and unconditional manner. **Employees** also move randomly, but accept only new positions with a lower function value than their current location on the hypersurface. Finally, **Onlookers** randomly probe the environment of Employees to locally accelerate the sampling frequency in promising areas. This approach has been benchmarked extensively^{35,36} and applied to global optimization problems in engineering^{37–40} and computer science^{41–44} with great success.

The success of the artificial bee colony algorithm for these types of optimization problems has led us to attempt to transfer the algorithm to optimization problems in physics and chemistry^{45,46} and, in particular, the optimization of molecular structure. However, preliminary geometry optimizations for small Lennard-Jones⁴⁷ clusters with 10–20 particles show that the original formulation of the algorithm^{34–36} may sometimes yield a relatively poor performance.

Our aim is to make the algorithm suitable for optimization of molecular and supramolecular potential energy surfaces without requiring atomic gradients and for systems with arbitrary symmetry. In particular, we want to minimize the potential energy E of N_P interacting particles.

II. MODIFIED ARTIFICIAL BEE COLONY ALGORITHM

We express the free variables of this optimization problem, i.e., the coordinates of the N_P particles ($\mathbf{R}_1, \mathbf{R}_2, \dots, \mathbf{R}_{N_P}$) as a single vector \mathbf{x} . We also define a fitness function to gauge the quality of a given structural

^{a)}Electronic mail: daniel.sebastiani@chemie.uni-halle.de.

configuration \mathbf{x} based on the total interaction energy $E(\mathbf{x})$,

$$f(E(\mathbf{x})) = \begin{cases} 1 - E(\mathbf{x}), & E(\mathbf{x}) < 0 \\ (1 + E(\mathbf{x}))^{-1}, & E(\mathbf{x}) \geq 0. \end{cases} \quad (1)$$

This transformation of the total energy into a fitness function is advantageous because in this way the fitness $f(E)$ is a strictly monotonically decreasing function of the energy E . Hence, minima of E correspond to maxima of $f(E)$. In addition $f(E)$ is by construction non-negative even for very condensed cluster structures with $E > 0$; further, $f(E)$ is invertible, and becomes maximal at the global minimum of the PES.

The optimization is now performed via the collective behavior of a population (or a swarm) of N_A random walkers (or agents/bees) A_i , which are associated to structural configurations \mathbf{x}_i and corresponding qualities f_i ,

$$A_i = (\mathbf{x}_i, f_i), \quad (2)$$

$$\mathbf{x}_i = (\mathbf{R}_1^{(i)}, \mathbf{R}_2^{(i)}, \dots, \mathbf{R}_{N_p}^{(i)}), \quad (3)$$

$$E_i = E(\mathbf{x}_i), \quad (4)$$

$$f_i = f(E_i). \quad (5)$$

In the following, we outline our modified ABC algorithm by means of its translation operators for the positions of the individual agents. In comparison with the original ABC scheme, we no longer repartition the ensemble of agents into classes of different behavior; instead, our agents are all equal but can adopt different propagation strategies (translation operators):

Free Move: The free move operator (FMO) places the agent at a fully random position on the PES. This behavior contributes to the exploratory character of the algorithm.

Local Move: The local move operator (LMO) propagates the calling agent locally within a given environment of its present position. At first, a random trial position is chosen within the close proximity of the agent's position \mathbf{x}_i by adding gaussian-distributed random numbers which are multiplied by a factor r_s . The agent accepts this trial position if the new fitness is better. Otherwise, the agent keeps its old position.

The choice of operator depends on the history of the calling agent. Initially, all agents are distributed randomly on the PES by the FMO. Afterwards, all agents use the LMO by default. Hence, the algorithm normally performs multiple Markovian downhill searches.

At some stage of such a downhill search, the number of failed moves will increase due to the proximity of the agent to a local minimum or saddle point. At this stage the displacement factor r_s is consecutively reduced after N_L failed moves for the particular agent. When a given lower threshold for r_s is reached, the FMO is enforced. This two-stage reaction is motivated by the fact that the fraction of the PES with better fitness becomes increasingly small in close proximity of a

local minimum. By reducing the displacement factor r_s , this fraction is amplified, and thus is the probability to make successful local moves near local minima.

So far, this approach resembles N_A simultaneous but independent Markovian downhill searches. The particular strength of the artificial bee colony algorithm, however, lies in the shared information on the positions of the agents on the PES and the focus on promising areas. This means that such areas on the PES with low energies are sampled in much more detail than the remaining parts. In case of our implementation, agents with low energies perform more move attempts than agents with higher energies. For this purpose, the algorithm repeats two different phases:

Employee phase: During this phase, all N_A agents call once the LMO or FMO depending on their current state. This phase ensures progress of all agents.

Onlooker phase: Here successful agents make additional calls to LMO or FMO. In this phase the computational resources for N_O additional calls are distributed to those agents that are in promising areas of the PES. The relative quality within the whole population determines if an agent is considered successful: the probability to be chosen for an additional move increases with the fitness of the agent according to

$$p_i = \frac{f_i}{\sum_{j=1}^{N_A} f_j}. \quad (6)$$

The cyclic repetition of the Employee and Onlooker phases is sketched in Figure 1. Every agent makes one move attempt during the Employee phase, which is either a local downhill move or a global reset to escape from a local minimum. In the Onlooker phase, agents with high relative fitness values make additional move attempts to accelerate the sampling of low energy areas on the potential energy surface.

III. RESULTS

We have applied the modified artificial bee colony algorithm to the problem of global geometry optimization of molecular clusters of 2–57 atoms. For the interatomic interaction, we use three of the most common potential types. In the following, we show the performance of our ABC algorithm during the optimization process with respect to the cluster size. For all systems, the parameters of the optimization algorithm are adjusted as a function of the number of particles in the cluster.

The exact settings are shown in Table I. As outlined above, N_A and N_O denote the numbers of agents in the swarm and Onlooker steps. N_L is the number of successively failed attempts to make a local move until the displacement factor r_s is reduced by a factor 0.5 and N_D denotes the maximum number of reductions of r_s before a free move is enforced. The initialization box B_0 defines the allowed range of cartesian coordinates of the particles for free moves. During the local downhill search the cartesian coordinates are not restricted. Thus, a cluster optimization starts from a very compact state, but is allowed to expand freely during the optimization.

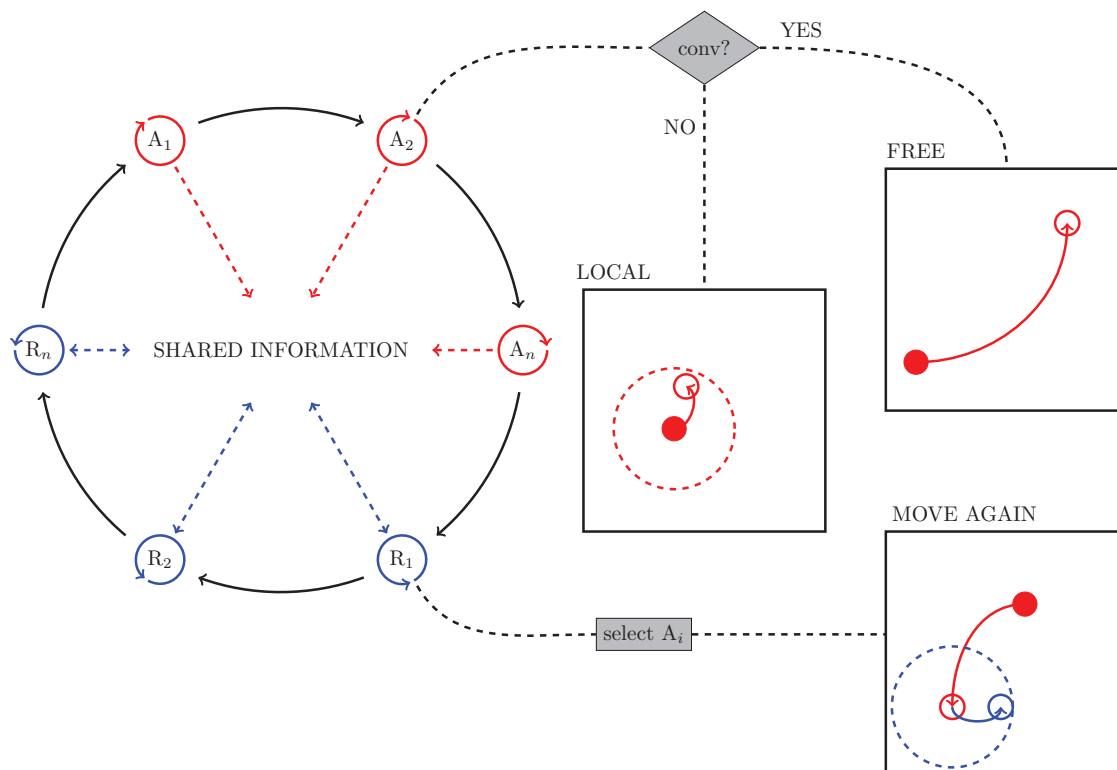


FIG. 1. Schematic description of the optimization cycle of the modified artificial bee colony algorithm.

To account for the stochastic nature of our optimization approach, we have performed a large number of independent optimizations for each cluster size and type of interaction potential. The performance of the algorithm is computed as the average. In particular, we present the mean computational cost that was necessary to locate the global minima on the PES. The reference global minima were taken from the Cambridge cluster database^{15,48–51} (CCD). The computational cost of a single optimization run is quantified by the total number of energy evaluations (single point calculations, SPC) during the optimization process.

A. Morse cluster

As first interaction potential, we optimized clusters of particles without internal structure using the purely distance-based Morse⁵² potential,

$$E(r_{ij}) = \epsilon e^{\phi(1-r_{ij}/r_0)}(e^{\phi(1-r_{ij}/r_0)} - 2). \quad (7)$$

The depth of the potential well ϵ and the pair equilibrium distance r_0 are set to 1 by convention. The parameter $\phi > 0$ determines the width and steepness of the potential well. Here we used three values which correspond to a very broad potential well ($\phi = 3$), a potential well with roughly the same cur-

vature as the Lennard-Jones⁴⁷ potential ($\phi = 6$) and a more narrow potential well ($\phi = 10$).

Figure 2 shows the computational cost for the optimization of Morse clusters with $N_p = 5, \dots, 19$ particles and $\phi = 3, 6, 10$; each data point was averaged over 1000 independent optimization runs. The mean computational cost scales roughly exponentially with the system size N_p . We observe that the computational cost is affected by the width of the potential well: with increasing ϕ (more short-sighted interaction, see Eq. (7)), the optimization becomes more expensive. This is in line with the common assumption that steep potential funnels render geometry optimizations more expensive. The standard deviations of the computational cost were of the same order of magnitude as the average.

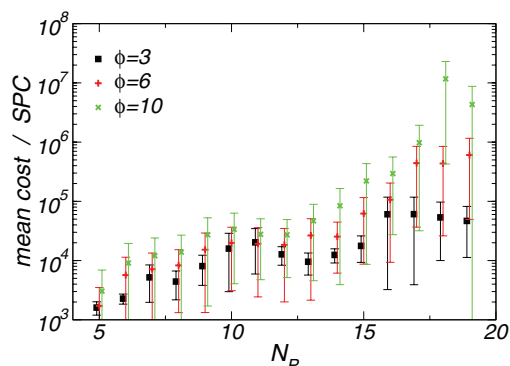


FIG. 2. Average cost and standard deviations in single point calculations for the global structural optimization of clusters of $N_p = 5, \dots, 19$ Morse⁵² particles with 1000 independent optimization runs each.

TABLE I. General settings for the modified artificial bee colony depending on the number of particles (N_p) in the cluster.

Agents	N_A	$2 \times N_p$	Displacement factor	r_s	0.01
Onlooker steps	N_O	$20 \times N_p$	Initialization box	B_0	$0.02 \times \sqrt[3]{N_p}$
Limit	N_L	$5 \times N_p$	Divisions	N_D	7

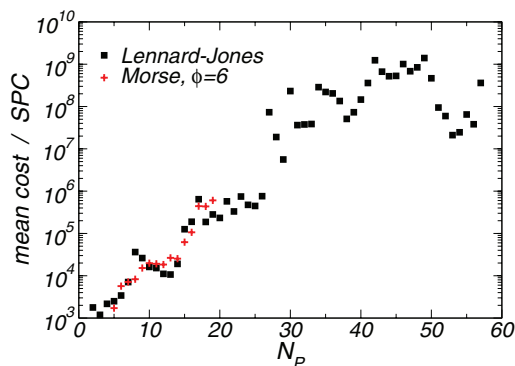


FIG. 3. Average cost in single point calculations for the global structural optimization of clusters of $N_p = 2, \dots, 57$ Lennard-Jones⁴⁷ particles with 200–1000 independent optimization runs each. For comparison, the corresponding data points for Morse⁵² particles (with $N_p = 5, \dots, 19$) are repeated from Figure 2.

Note that our implementation assumes convergence only at the energy value of the global minimum structure known from the CCD.

B. Lennard-Jones cluster

We have extended our analysis to molecular clusters of up to 57 particles interacting via a Lennard-Jones⁴⁷ potential,

$$E(r_{ij}) = 4\epsilon \left(\frac{\sigma^{12}}{r_{ij}^{12}} - \frac{\sigma^6}{r_{ij}^6} \right). \quad (8)$$

Again, we employed reduced variables ($\epsilon = \sigma = 1$). For small clusters $N_p \leq 25$, we averaged over 1000 independent optimization runs. Bigger clusters were averaged over 200 runs.

Figure 3 shows the average cost for the optimization of cluster structures with 2, ..., 57 particles. As in the case of the Morse clusters, the average cost scales roughly exponentially with the system size N_p ; the overall scale is comparable. For bigger clusters ($N_p > 25$), we observe large fluctuations in the computational costs between clusters of similar sizes. Again, the standard deviations of the computational costs are roughly of the same order as the shown averaged values.

Interestingly, the cluster with $N_p = 38$, which is commonly assumed a difficult optimization case due to a steep double-funnel⁵³ turned out to be a comparable easy case for our modified ABC algorithm.

C. TIP5P cluster

We finalized our analysis with the geometry optimization of a series of clusters of water molecules, which have an internal structure (see Figure 5 for a cluster with six molecules). We used a rigid water model, specifically the five point transferable intermolecular potential (TIP5P),⁵⁴ the potential energy of two molecules a and b is given by

$$E_{a,b} = \frac{e^2}{4\pi\epsilon_0} \sum_i \sum_j \frac{q_i q_j}{r_{ij}} + 4\epsilon \left(\frac{\sigma^{12}}{r_{OO}^{12}} - \frac{\sigma^6}{r_{OO}^6} \right). \quad (9)$$

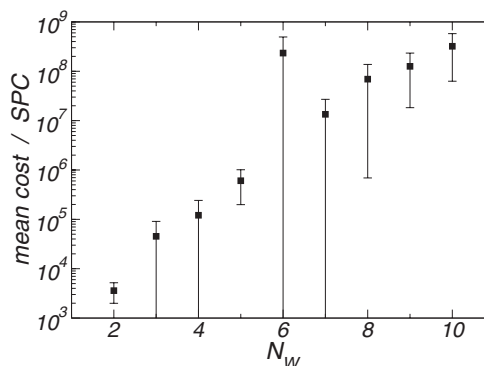


FIG. 4. Average cost and standard deviation in single point calculations for the global structural optimization of clusters of $N_w = 2, \dots, 10$ TIP5P⁵⁴ water molecules with 31–1000 independent optimization runs each.

This type of potential combines a Coulomb interaction with charges $q = \pm 0.241$ (relative to the elementary charge e) located on the hydrogen atoms and the sites of the lone pair electrons of the oxygen atom, as well as a van der Waals term, with the energy scale $\epsilon = 0.66944$ kJ mol⁻¹ and length scale $\sigma = 3.12$ Å. The variable r_{ij} denotes the intermolecular distances between the charged sites and r_{OO} is the distance between the oxygen atoms. For the setting of the optimization algorithm, we use $N_p = 3 \times N_w$, with N_w being the number of water molecules.

The mean computational cost is shown in Figure 4. We used a sample size of 1000 independent optimizations for the smaller clusters 2, ..., 5 and the cluster with 7 water molecules. The bigger clusters were averaged over 31–242 independent runs. Except for the cluster with $N_w = 6$ water molecules, we observe a perfect exponential scaling with the system size.

Regarding the cluster with six water molecules, which is known to be hard to optimize,^{55,56} we have observed that our algorithm got trapped in a local minimum at $E \approx -195.8$ kJ mol⁻¹ after typically 5×10^6 single point calculations, which would correspond to the interpolated computational cost for $N_w = 6$. While the algorithm still converged to the referenced global minimum at $E \approx -197.9$ kJ mol⁻¹ during all the optimization runs, the optimal structure was extremely difficult to reach. Both minima are shown in Figure 5.

Although the $N_w = 6$ water cluster is the only system for which our modified ABC algorithm experienced such difficulties, this case illustrates that the optimization of supramolecular structures with complex interaction types can be unpredictable in terms of the required optimization effort. Note that a convergence criterion based on stagnation at a particular conformation would have led to a structure (Figure 5, left) that is energetically more than 2 kJ mol⁻¹ above the global minimum (Figure 5, right).

IV. DISCUSSION

We have presented a modification of the artificial bee colony algorithm, a stochastic optimization approach from the field of swarm intelligence. We have applied our algorithm to the global geometry optimization of molecular cluster

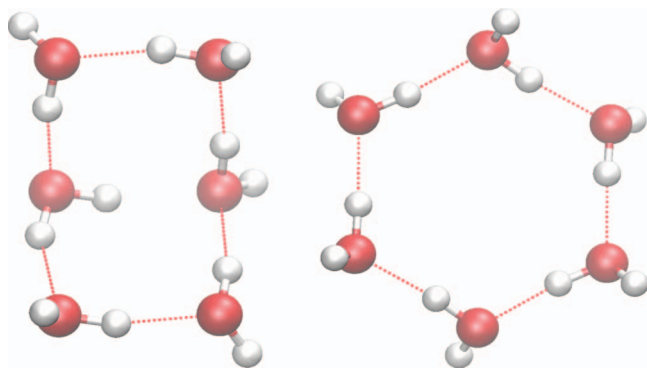


FIG. 5. Stable clusters of six rigid water molecules interacting via the TIP5P⁵⁴ potential: a local minimum at $E = -195.777$ kJ mol⁻¹ that often appeared during the optimizations (left); the global minimum as referenced in the Cambridge cluster database,^{48,51} $E = -197.9372$ kJ mol⁻¹ (right).

structures for three different potential types. The algorithm is fully unbiased and does not rely on atomic gradients. We have shown that our algorithm is able to find the global minima on the potential energy surfaces for every system size and potential type at a computational cost that scales exponentially with the number of particles.

Note that the absolute cost is presently sizeably above that of competing approaches such as minima hopping. Nevertheless, we believe that further improvements of our ABC algorithm can considerably speed up its convergence. In particular, the use of gradient-based local minimization techniques will greatly enhance the performance near a local minimum. We are presently adding this feature to our implementation. In the present study, we have used a stable but not specifically tuned setting for the algorithm (see Table I). We are currently studying the influence of these control parameters on the performance of the algorithm.

However, we believe already now that the artificial bee colony algorithm represents a competitive member among the currently established schemes for the global optimization of molecular structures.

ACKNOWLEDGMENTS

This work has been supported by the German Research Foundation (DFG) under Grant Nos. SE 1008/5 and SE 1008/6. Computing infrastructure was provided by the Northern German Supercomputing Alliance (HLRN) under Grant No. HLRN/bec00082.

D.S. would like to thank the Max Planck Graduate Center. T.D.K. acknowledges financial support from the MAINZ Graduate School of Excellence and the IDEE project of the Carl Zeiss Foundation.

¹J. Maddox, *Nature* **335**, 201 (1988).

²W. van Gunsteren, *Protein Eng. Des. Sel.* **2**, 5 (1988).

³J. D. Bryngelson, J. N. Onuchic, N. D. Socci, and P. G. Wolynes, *Proteins* **21**, 167 (1995).

⁴W. F. van Gunsteren, D. Bakowies, R. Baron, I. Chandrasekhar, M. Christen, X. Daura, P. Gee, D. P. Geerke, A. Glättli, P. H. Hünenberger, M. A. Kastenholtz, C. Oostenbrink, M. Schenk, D. Trzesniak, N. F. A. van der Vegt, and H. B. Yu, *Angew. Chem., Int. Ed. Engl.* **45**, 4064 (2006).

⁵M. Christen and W. F. van Gunsteren, *J. Comput. Chem.* **29**, 157 (2008).

⁶U. H. Hansmann, *Chem. Phys. Lett.* **281**, 140 (1997).

⁷S. Kirkpatrick, C. D. Gelatt, and M. P. Vecchi, *Science* **220**, 671 (1983).

⁸R. C. van Schaik, W. F. van Gunsteren, and H. J. Berendsen, *J. Comput.-Aided Mol. Des.* **6**, 97 (1992).

⁹J. Lee, H. A. Scheraga, and S. Rackovsky, *J. Comput. Chem.* **18**, 1222 (1997).

¹⁰A. Laio and M. Parrinello, *Proc. Natl. Acad. Sci. U.S.A.* **99**, 12562 (2002).

¹¹M. Iannuzzi, A. Laio, and M. Parrinello, *Phys. Rev. Lett.* **90**, 238302 (2003).

¹²R. Martoňák, A. Laio, and M. Parrinello, *Phys. Rev. Lett.* **90**, 075503 (2003).

¹³S. Goedecker, *J. Chem. Phys.* **120**, 9911 (2004).

¹⁴S. Goedecker, W. Hellmann, and T. J. Lenosky, *Phys. Rev. Lett.* **95**, 055501 (2005).

¹⁵D. J. Wales and J. P. K. Doye, *J. Phys. Chem. A* **101**, 5111 (1997).

¹⁶J. P. K. Doye, D. J. Wales, and M. A. Miller, *J. Chem. Phys.* **109**, 8143 (1998).

¹⁷D. J. Wales and H. A. Scheraga, *Science* **285**, 1368 (1999).

¹⁸S. Stepanenko and B. Engels, *J. Comput. Chem.* **28**, 601 (2007).

¹⁹S. Stepanenko and B. Engels, *J. Comput. Chem.* **29**, 768 (2008).

²⁰S. Stepanenko and B. Engels, *J. Phys. Chem. A* **113**, 11699 (2009).

²¹C. Grebner, J. Becker, S. Stepanenko, and B. Engels, *J. Comput. Chem.* **32**, 2245 (2011).

²²A. R. Oganov and C. W. Glass, *J. Chem. Phys.* **124**, 244704 (2006).

²³G. Böhm, *Biophys. Chem.* **59**, 1 (1996).

²⁴R. C. Glen and A. W. R. Payne, *J. Comput.-Aided Mol. Des.* **9**, 181 (1995).

²⁵C. Roberts, R. L. Johnston, and N. T. Wilson, *Theor. Chem. Acc.* **104**, 123 (2000).

²⁶L. D. Lloyd, R. L. Johnston, C. Roberts, and T. V. Mortimer-Jones, *ChemPhysChem* **3**, 408 (2002).

²⁷S. Darby, T. V. Mortimer-Jones, R. L. Johnston, and C. Roberts, *J. Chem. Phys.* **116**, 1536 (2002).

²⁸J.-O. Joswig and M. Springborg, *Phys. Rev. B* **68**, 085408 (2003).

²⁹M. Springborg, Y. Dong, V. G. Grigoryan, V. Tevekelyiska, D. Alamanova, E. Kasabova, S. Roy, J.-O. Joswig, and A. M. Asaduzzaman, *Z. Phys. Chem.* **222**, 387 (2008).

³⁰V. A. Frolov and K. Reuter, *Chem. Phys. Lett.* **473**, 363 (2009).

³¹Z. E. Brain and M. A. Addicoat, *J. Chem. Phys.* **135**, 174106 (2011).

³²R. Martoňák, A. R. Oganov, and C. W. Glass, *Phase Transitions* **80**, 277 (2007).

³³S. E. Schönborn, S. Goedecker, S. Roy, and A. R. Oganov, *J. Chem. Phys.* **130**, 144108 (2009).

³⁴D. Karaboga and B. Basturk, *J. Global Optim.* **39**, 459 (2007).

³⁵D. Karaboga and B. Basturk, *Appl. Soft Comput.* **8**, 687 (2008).

³⁶D. Karaboga and B. Akay, *Appl. Math. Comput.* **214**, 108 (2009).

³⁷R. Venkata Rao and P. J. Pawar, *Appl. Soft Comput.* **10**, 445 (2010).

³⁸J. M. S. de Oliveira and R. Schirru, *Ann. Nucl. Energy* **38**, 1039 (2011).

³⁹S. Samanta and S. Chakraborty, *Eng. Applic. Artif. Intell.* **24**, 946 (2011).

⁴⁰M. Sonmez, *Appl. Soft Comput.* **11**, 2406 (2011).

⁴¹A. Singh, *Appl. Soft Comput.* **9**, 625 (2009).

⁴²S. Sundar and A. Singh, *Inf. Sci. (N.Y.)* **180**, 3182 (2010).

⁴³T.-J. Hsieh, H.-F. Hsiao, and W.-C. Yeh, *Appl. Soft Comput.* **11**, 2510 (2011).

⁴⁴R. Zhang and C. Wu, *Entropy* **13**, 1708 (2011).

⁴⁵C. Schiffmann and D. Sebastiani, *J. Chem. Theory Comput.* **7**, 1307 (2011).

⁴⁶A. C. Ihrig, C. Schiffmann, and D. Sebastiani, *J. Chem. Phys.* **135**, 214107 (2011).

⁴⁷J. E. Jones, *Proc. R. Soc. London, Ser. A* **106**, 463 (1924).

⁴⁸D. J. Wales, J. P. K. Doye, A. Dullweber, M. P. Hodges, F. Y. Naumkin, F. Calvo, J. Hernández-Rojas, and T. F. Middleton, The Cambridge Cluster Database (2012), see <http://www-wales.ch.cam.ac.uk/CCD.html>.

⁴⁹J. P. K. Doye, D. J. Wales, and R. S. Berry, *J. Chem. Phys.* **103**, 4234 (1995).

⁵⁰J. P. K. Doye and D. J. Wales, *J. Phys. B* **29**, 4859 (1996).

⁵¹T. James, D. J. Wales, and J. Hernández-Rojas, *Chem. Phys. Lett.* **415**, 302 (2005).

⁵²P. Morse, *Phys. Rev.* **34**, 57 (1929).

⁵³J. P. K. Doye, M. A. Miller, and D. J. Wales, *J. Chem. Phys.* **110**, 6896 (1999).

⁵⁴M. W. Mahoney and W. L. Jorgensen, *J. Chem. Phys.* **112**, 8910 (2000).

⁵⁵B. Santra, A. Michaelides, M. Fuchs, A. Tkatchenko, C. Filippi, and M. Scheffler, *J. Chem. Phys.* **129**, 194111 (2008).

⁵⁶C. Pérez, M. T. Muckle, D. P. Zaleski, N. A. Seifert, B. Temelso, G. C. Shields, Z. Kisiel, and B. H. Pate, *Science* **336**, 897 (2012).